arXiv:cond-mat/0506380v1 [cond-mat.mtrl-sci] 15 Jun 2005

Contributions to the mixed–alkali effect in molecular dynamics simulations of alkali silicate glasses

Heiko Lammert* and Andreas Heuer†
Institute of Physical Chemistry and Sonderforschungsbereich 458, Corrensstr. 30, D-48149 Münster, Germany
(Dated: March 23, 2022)

The mixed–alkali effect on the cation dynamics in silicate glasses is analyzed via molecular dynamics simulations. Observations suggest a description of the dynamics in terms of stable sites mostly specific to one ionic species. As main contributions to the mixed–alkali slowdown longer residence times and an increased probability of correlated backjumps are identified. The slowdown is related to the limited accessibility of foreign sites. The mismatch experienced in a foreign site is stronger and more retarding for the larger ions, the smaller ions can be temporarily accommodated. Also correlations between unlike as well as like cations are demonstrated that support cooperative behavior.

I. INTRODUCTION

The disordered network structure of glasses provides a highly complex environment for the transport of mobile ions. A basic consensus has developed that the ionic motion consists of jumps between distinct minima of the energy landscape[1,2]. Because of the strong Coulomb interaction between the ions the effective energy landscape will perpetually change with the motion of the ions. The dispersion in the frequency dependence of ionic conductivity can be interpreted[3,4] as a consequence of correlated backward jumps forced by the interaction with other ions.

The complexity of the ion dynamics in glasses is highlighted by the mixed–alkali effect[5,6]: In glasses containing two different alkali species, a deep minimum in the mobility of the ions is observed. Even small concentrations of a second alkali species effectively slow down the total ion dynamics.

Several important structural properties of mixed–alkali (MA) glasses are already known. EXAFS measurements[7] have established that the cations retain the same specific coordination environments as in single–alkali (SA) glasses. This was also supported by reverse Monte Carlo calculations[8]. Furthermore, NMR measurements[9,10] have shown that the different alkali cations are intimately mixed on the microscopic scale and do not belong to phase segregated parts.

Specific information about the dynamics of cations in disordered ion conductors can be obtained via Molecular Dynamics (MD) simulations. For SA glasses it has been shown that regions of high ionic mobility form channels[11,12] that arise statistically[11,12,13]. Proof for some structure at the scale of these channels can also be found in measurements of the dynamic structure factor[14,15]. One of the most important MD results for MA glasses is the observation that ions only rarely jump into sites vacated by the other species[16] and that the site characteristics of both species are very different[17,18,19].

Several models[8,20,21], inspired by the observations of site selectivity, feature distinct sets of adapted sites for each alkali species. Taking the site selectivity as a starting point one may ask whether the dynamics in the MA system of composition $(A_2O)_a(B_2O)_b(SiO_2)_{1-a-b}$ can be viewed as the *independent* superposition of two SA systems $(A_2O)_a(SiO_2)_{1-a}$ and $(B_2O)_b(SiO_2)_{1-b}$, respectively. If this were true the dramatic decrease of the dc conductivity in the MA system would be related to the well-known observation that the alkali dynamics in SA systems become much slower for lower alkali concentration and one might just speak of a dilution effect.

Experimental results tell that reality is more complex. For example, in recent measurements of dc conductivities and tracer diffusivities in Na–Rb–borate glasses the mobility of sodium and rubidium is compared to that in pure Na–borates and Rb–borates with identical alkali content[22]. Despite a significant decrease of the conductivity for the ternary glasses the conductivity is still significantly larger than the sum of those in the respective SA glasses. Furthermore, the experimental data reveal asymmetric behavior with respect to the two alkali species. A dramatic difference is visible when comparing the limit where the smaller ion (here:Na) is the minority species as compared to the opposite limit. It turns out that the small ion as minority species is still relatively mobile and its diffusion constant, as determined by tracer diffusion experiments, only weakly depends on concentration. In contrast, in the other limit the large ion becomes immobile. Similar observations have been already made in earlier experiments; see e.g.[5,23].

A simple reason for the apparent increase of mobility in mixed alkali systems as compared to the sum of the individual glasses may be given by the different network structures. Due to the higher alkali content in the mixed–alkali system the network structure is more discontinuous, giving rise to higher network mobility and thus, possibly, to higher alkali mobility.

Beyond this effect it is discussed whether the adaption of the individual sites may change with time. The rearrangement of free volume has been put forward as a possible mechanism for the readaption, based on measurements of the pressure dependence of ionic conductivity[24,25]: A site entered by a too large ion has to expand, while a site entered by a smaller ion can shrink. If both happens at the same time in close vicinity, an isochoric redistribution of site volume via relaxations of

the matrix could facilitate the readaption of both sites. If this mechanism of *matrix mediated coupling* were indeed present, an important correlation between the unlike cations would be a present in the MA system[25].

Actually, the presence of the release of mismatches and thus the readaption of sites in the glassy phase has been already postulated in the Dynamic Structure Model[21]. Others suppose that the adaption of a site is definitively fixed during the glass transition[8]. In a very different approach it is assumed that a distribution of sites is open in principle to all ions[26,27]. In this class of models, the competition for favorable sites is governed by the different radii of the cation species.

The goal of our work is to elucidate the mechanism of ion dynamics in mixed–alkali systems via MD simulations on a microscopic level. The analysis is based on our method[28] to identify individual ionic sites from the MD trajectories ; see also[29]. This procedure was also successfully applied to simulations of phosphate glasses[30] and rationalized in more general terms[31]. In this investigation, the method is for the first time applied to a MA system. From comparison of the dynamics in SA systems and MA systems, three major aspects will be treated. First, the site selectivity is quantified in detail. Second, the trajectories of the alkali ions are characterized and compared with the typical behavior in SA systems. Third, dynamic correlations between like and unlike cations are analyzed.

II. TECHNICAL ASPECTS

We performed molecular dynamics simulations of alkali silicate glasses $x(\mathrm{K_2O}) \cdot (1-x)(\mathrm{Li_2O}) \cdot 2(\mathrm{SiO_2})$ with $x = 0.0, 0.5, 1.0$. We use a modified version of the software MOLDY[32], using Buckingham–type pair potentials developed by Habasaki *et al.*[33], that are well tested for comparable systems[34,35,36]. The simulations were done in the NVT–ensemble, with systems of 1215 particles, i.e. 270 alkali ions. The size of the simulation boxes was set according to experimental densities[37], resulting in $V(x=0) : V(x=0.5) : V(x=1) = 1 : 1.03 : 1.06$. In[33] the experimental densities for the two SA systems could be reproduced from NpT-simulations at identical pressure. In contrast, we obtain differing pressures in our NVT runs with these experimental densities. At $T = 3000$K, where equilibrium runs are easily possible, the pressure of the two limiting systems for our simulations are $p(x=0) \approx 2.5$ GPa and $p(x=1) \approx 4.7$ GPa. Yet the pressure of the MA system is roughly the average of the two limiting SA systems, with a deviation of 0.4 ± 0.2 GPa. This relation does not change at different temperatures. The additive behavior supports the idea that the observed slowdown in the MA system (see below) is not generated by our choice of densities.

The systems were prepared at high temperatures and cooled down in steps. Here we present data from runs at 850K, which is well below the glass transition. The alkali subsystem was equilibrated at this temperature for 40ns.

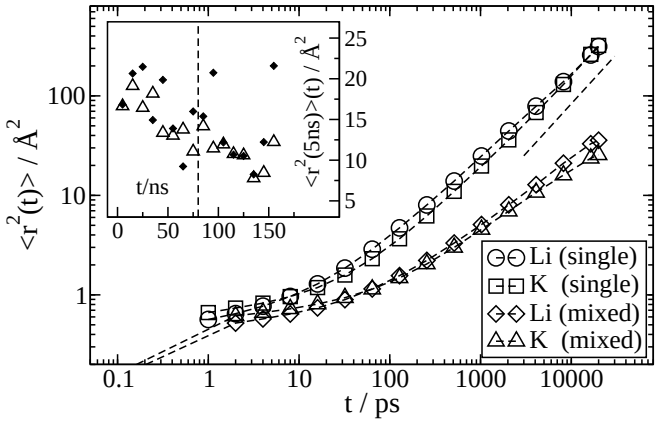


FIG. 1: Mean square displacements of alkali ions in single and mixed–alkali systems. Inset: Time dependence of $< r^2(5\mathrm{ns}) >$ in the mixed–alkali system. The broken line at 80ns indicates that for this work only information from the second part of our data is taken if not mentioned otherwise.

Subsequently trajectories were generated over 40ns for the SA glasses, and over 160ns for the MA system. The determination of cation sites based on cation trajectories is described in detail in[28].

III. RESULTS

A. General dynamics

Simulations below the computer glass transition temperature have to be carefully conducted due to expected aging effects of the network. Furthermore one may expect that due to this effect also the lithium dynamics will somewhat change with time. After an initial simulation period of 40ns we have calculated the mean square displacement during time intervals $[t_0, t_0 + 5\mathrm{ns}]$ where different starting times t_0 during our production run of 160 ns have been chosen; see inset of Fig. 1. During the first 80ns a significant slowdown is present, which is less visible for the second 80ns. Thus one finds a dynamic signature of network aging effects. Of course, subsequent aging effects of the network will still be present, but probably on longer time scales. The subsequent analysis is mainly performed for the second half of our production run. In any event, all general conclusions drawn in this work could already be obtained from analyzing just the first half of the production run.

Figure 1 shows the mean square displacements of the alkali cations in both the SA and MA glasses. In the long time limit the ionic transport becomes diffusive, corresponding to a slope of one in the double logarithmic plot. In the SA glasses this is reached around $t = 10$ns. The diffusivities at 850K in the SA systems are $D_{Li} = 2.9 \times 10^{-7}\mathrm{cm^2 s^{-1}}$ and $D_K = 2.6 \times 10^{-7}\mathrm{cm^2 s^{-1}}$. The curves for lithium and potassium in the MA system do not attain a slope of one during the time interval shown.

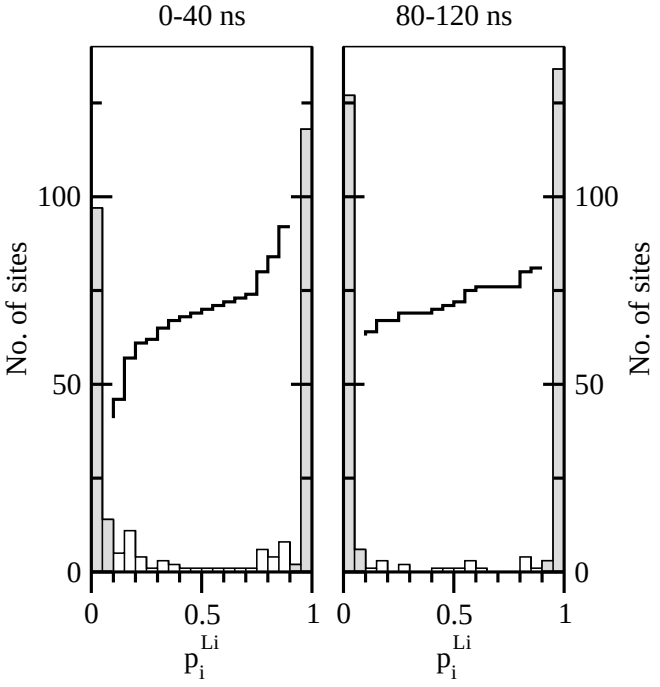


FIG. 2: Distribution of p_i^{Li}, the fraction of time a site is occupied by lithium cations. This is a measure of specificity (see text). The shaded areas correspond to adapted sites, characterized by specificities ≥ 0.9. The bold black lines give the cumulative sum over the number of mixed sites, shifted in vertical direction for convenience.

This observation is in agreement with earlier findings in SA glasses, where we noted that the diffusive regime is reached only for larger values of the mean square displacement in systems with lower alkali content[28]. Under the assumption of time-temperature superposition and the ability to reach the linear regime at higher temperatures we may estimate the diffusion constants as $D_{Li} = 2.8 \times 10^{-8}\mathrm{cm}^2\mathrm{s}^{-1}$ and $D_K = 1.9 \times 10^{-8}\mathrm{cm}^2\mathrm{s}^{-1}$. The slowdown of the diffusivities as compared to the single alkali systems then amounts to a factor of ≈ 10 for lithium and ≈ 14 for potassium.

B. Properties of ion sites

By mapping the trajectories of the cations onto the sites obtained from our analysis, jumps between the sites can be identified. As in our previous work, we registered a jump if an ion leaves a site and moves into a different one. The duration of an ion's residence in a site, denoted τ_{res}, is defined by the time between its jump into the site and the subsequent jump out of it. When an ion leaves a site and returns without reaching a different site, the residence is not interrupted. In total we find 288 sites. Thus, there are ca. 8% more sites than ions. This small excess number is close to the result for the SA system[28].

¿From the residence data it is also possible to calculate the average occupation o_i for each site i. In the MA system we distinguish the contributions o_i^M of the different cations $M = \{\mathrm{Li}, \mathrm{K}\}$. The specificity of a site can be quantified by $p_i^{\mathrm{Li}} = o_i^{\mathrm{Li}}/(o_i^{\mathrm{Li}} + o_i^{\mathrm{K}})$ and $p_i^{\mathrm{K}} = 1 - p_i^{\mathrm{Li}}$, the probabilities that an occupying ion is lithium or potassium, respectively. One can define the specificity s_i=max$(p_i^{\mathrm{Li}}, p_i^{\mathrm{K}})$ as the larger of both p_i^M. The distribution of p_i^{Li} is shown in Fig. 2, for the interval $80-120$ns and also for $0-40$ns for comparison. The qualitative result is identical. At both times most sites have an $s_i \geq 0.9$, signalling a high specificity for one predominant ion. For the subsequent analysis these sites will be termed *adapted* sites or, alternatively, lithium or potassium sites. Those with lower specificity shall be called *mixed* sites. The regions corresponding to adapted sites are shaded in Fig. 2. Also shown are the cumulative sums over the number of mixed sites, shifted to a convenient vertical position. They clearly show that the number of mixed sites has decreased at the later time. Especially mixed sites with a s_i already close to 0.9 have vanished, with a corresponding increase in the number of adapted sites. At $80-120$ns, 94% (270) of all sites have a $s_i \geq 0.9$, compared to 82% (231) at $0-40$ns. 25% of all sites have been exclusively populated by lithium cations, and 19% have only been visited by potassium cations between $80-120$ns. The values for $0-40$ns are slightly lower again, being 23% and 17%, respectively. The differences between the time slices illustrate the effects of aging on our data.

The observed dependence of site specificity on simulation time rationalizes the observed time dependence of alkali mobility in the MA system. For later times the site specificity is more pronounced and thus the MA effect, expressed by a slowing down of the alkali dynamics, increases.

C. Site properties

In previous work on a SA system we have shown that the time scale it takes for an ion to hop from one equilibrium position to a nearby position is very short (less than 1 ps for lithium)[38]. This time scale is denoted t_{ch}. Furthermore, it turned out that on average a site was filled very soon after it was left by an ion. This is quantified by τ_{free}. The low values reflect the fact that the number of free sites is very small. We have determined the cumulative distribution $S(t)$ of both quantities for both the SA and the MA system. Thus, $S(t)$ expresses the probability, that a value $\leq t$ is found. The results are shown in Fig. 3.

For both systems it turns out that both times belong to the ps-time scale. Of course, the short transition times t_{ch} directly imply that ionic transitions are exclusively between adjacent sites. There is no long-range ionic motion through the network before entering a new site. Interestingly, in the SA system the potassium dynamics between two sites is nearly a factor of 10 slower than the

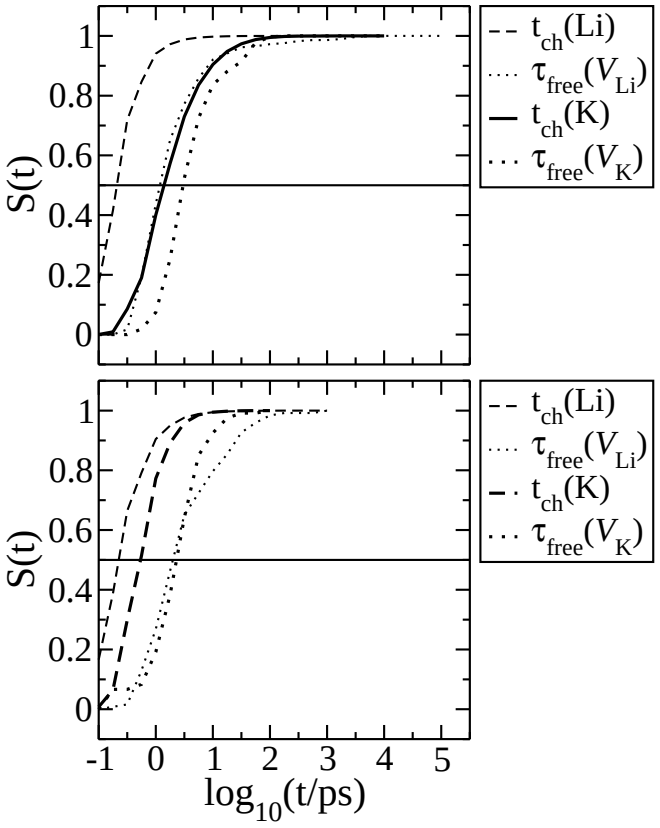


FIG. 3: Distributions of duration of jumps t_{ch} and of τ_{free}, the time a site stays unoccupied. Top: single–alkali systems; Bottom: mixed–alkali system. From the horizontal line with value 0.5 the median can be read off.

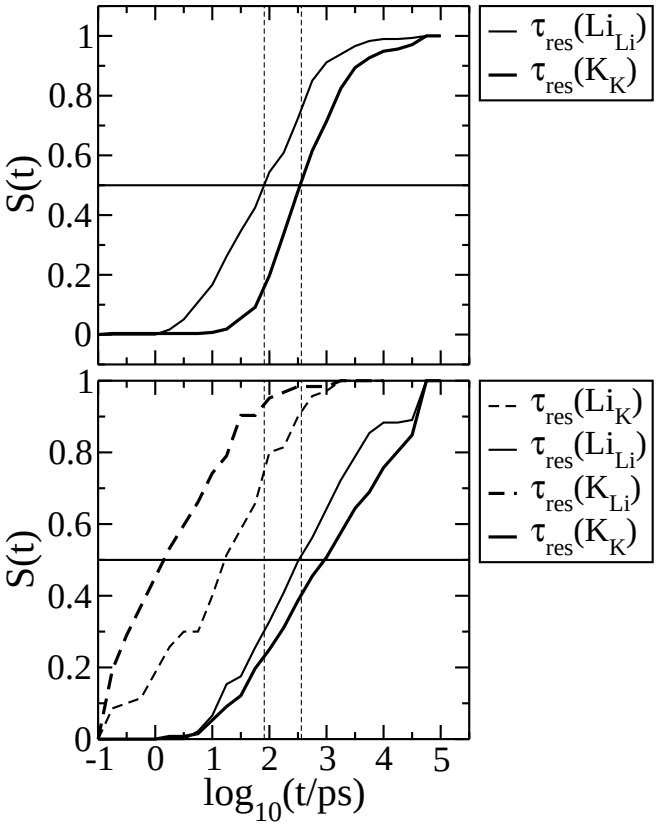


FIG. 4: Distributions of residence times τ_{res}. Top: single–alkali systems; Bottom: mixed–alkali system.

lithium dynamics. This difference alone cannot be explained only by the mass ratio of potassium and lithium. Actually, it becomes smaller in the MA system. It may come as a surprise that the time τ_{free} during which a site is vacant is not much longer than the transition time t_{ch} between adjacent sites. This reflects strongly cooperative dynamics, as stressed in previous simulation work[19,39]. Interestingly, the distributions are significantly broader for the MA system. This is a first hint that the dynamics is more heterogeneous in the MA system.

In the next step we calculate for every site its residence time, averaged over all ionic visits of this site. In the MA case we distinguish whether the visit is in a matched site or a mismatched site. Thus, $\tau_{res}(\mathrm{Li_K})$ corresponds to the waiting time of a lithium ion in a potassium site (characterized by $p_i^{\mathrm{Li}} < 0.1$). In Fig. 4 we show the corresponding cumulative distributions $S(t)$. Comparing the data from the SA systems shown in the top part with those of the MA system ($\tau_{res}(\mathrm{Li_{Li}})$ and $\tau_{res}(\mathrm{K_K})$, respectively) it turns out that the distribution is significantly broader in the latter case, in particular for long times. This means that the dynamics is more heterogeneous in the MA system. Actually, from previous work we know that the width of the distribution of residence times in the SA case does not depend on concentration[28]. Thus, the increasing relevance of dynamic heterogeneities in the MA case is our first observation, for which the dynamics displays qualitatively new features in MA systems as compared to SA systems. Interestingly, the median values of the distributions of residence times increase by a factor of only ca. three in the MA system. Thus the increase in residence times is not sufficient to explain the total extent of the MAE (factor 10-14, see above).

¿From Fig. 1 one can see that for the SA system the crossover to diffusive dynamics occurs on time scales somewhat longer than 100 ps. Here we define crossover such that the extrapolation from the long-time diffusive behavior deviates by a factor of 2 from the actual mean square displacement. This time scale is close to the median of the waiting times. Thus one may conclude that for the SA system the dynamics of ions from the slower half of the sites is not important for understanding the long-range transport. In contrast, for the MA case this crossover time can be estimated to be significantly beyond 10 ns. This implies that nearly the whole range of residence times is relevant for diffusive transport.

So far we have analyzed the behavior of matched events, i.e. adapted sites hosting the appropriate ion. Analyzing the waiting times for mismatched events we find, in particular for potassium, a strong reduction of the waiting times. This asymmetry in the behavior of lithium and potassium is also mirrored by the lower number of

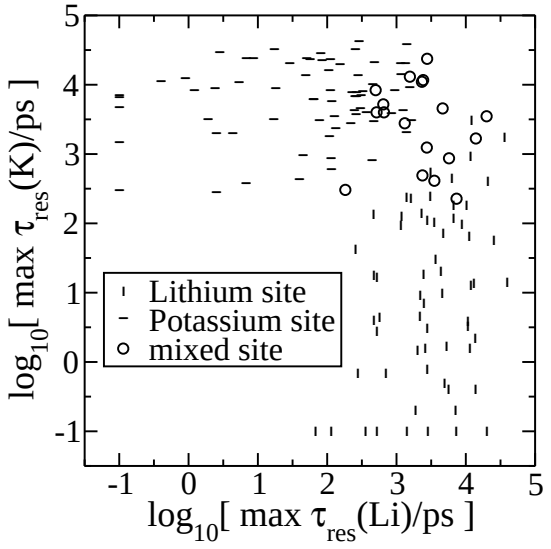


FIG. 5: Maximum residence times in sites visited by lithium and potassium ions during the simulation. For each site, the value for potassium is plotted versus the value for lithium. Adapted sites and mixed sites are distinguished by their relative occupation.

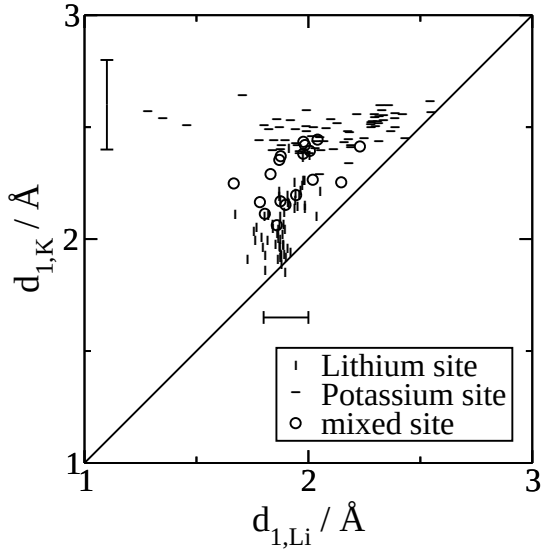


FIG. 6: The mean distance from a site to the closest oxygen during potassium residences, i.e. $d_{1,K}$, is plotted versus the value found during lithium residences in the same site, i.e. $d_{1,Li}$. The bars give the typical ranges of values for sites visited by only one species.

exclusive potassium sites mentioned in the discussion of Fig. 2. Qualitatively, this may be related to the fact that it is difficult for a potassium ion to enter a smaller lithium site. A more quantitative version of this argument will be presented below.

Although residences for mismatched events are on average significantly shorter than the residences found in matching events, the ranges covered by the distributions in Fig. 4 are overlapping. The duration of mismatching events can thus reach time scales normally present in well adapted sites. This possibility is explored in Fig. 5. For each site that has been visited by both lithium and potassium ions, the maximum residence time of a potassium ion is plotted against the maximum residence time of a lithium ion in the same site. Values for lithium sites, defined as above by $p_i^{\mathrm{Li}} > 0.9$, are noted as vertical lines, potassium sites as horizontal lines. Mixed sites are shown as circles.

The few mixed sites allow long maximum residence times for both species of ions, with values of at least 100ps, but typically reaching several ns for at least one species. All the adapted sites show residence times in this range for ions of the favored kind. The maximum residence time of a mismatched ion can be very short. But surprisingly, the possible residence times of mismatching events too cover the whole range of values up to comparable maximum time scales for both species, despite the high specificity of the respective sites. Even some strongly adapted sites seem thus to have the potential to accommodate ions of both species for a long time.

As a further step it is instructive to analyze the structural aspects of site specificity. The oxygen coordination environment of lithium and potassium sites is very different. One finds 4.5 oxygens up to $r \leq 2.87$Å for a lithium site and 10 at $r \leq 4.01$Å for a potassium site. The distances correspond to the first minima of the distribution function. A different way to characterize the differences is the observation that around a lithium ion, on average, three coordinating oxygen atoms are closer than 2.3 Å, while on average all coordinating oxygen atoms are further apart around a potassium ion. We determined for each site the mean distances $d_{i,M} (i = 1, 2, 3, 4; M = \mathrm{Li}, \mathrm{K})$ between the center of the site and the i-th closest oxygen atom whenever this site was either occupied by a lithium or a potassium ion. In particular $d_{1,M}$ is an extremely sensitive quantity to the local structure of a site. In Fig. 6 $d_{1,K}$ is plotted vs. $d_{1,Li}$ for all sites that have been visited by ions of both species. Again, data for lithium sites, for potassium sites and for mixed sites are distinguished by different symbols. The ranges of typical values for pure sites which are exclusively occupied by lithium or potassium, respectively, are given by the bars parallel to the respective axis. The bars cover more than 90 % of the values. In Tab. I we have for all combinations between ions and sites compiled the intervals for $d_{1,M}$ which apply to 68% of all sites.

Several interesting conclusions can be drawn about the distance to the next oxygen atom from Fig. 6 and the corresponding data of Tab. I. First we discuss the properties of adapted sites. (1) Except for a single site one has $d_{1,Li} < d_{1,K}$. This is a natural consequence of the different radii of the two ion species. (2) The median of $d_{1,Li}$ and even the total distribution is very similar when comparing pure sites with adapted sites, which at least once have hosted a potassium site. Thus the occasional occupation by potassium ions does not change

	Li site	K site	pure Li site	pure K site
Li ion	[1.83,1.94]Å	[1.87,2.33] Å	[1.84,1.93]Å	-
K ion	[1.93,2.20]Å	[2.43,2.60]Å	-	[2.47,2.64]Å

TABLE I: The intervals for the distance of the center of a site to the nearest oxygen where 68% of all cases are included. Only adapted sites are taken into account.

the local structure of a lithium site. (3) The reverse is not true. Pure potassium sites have on average larger values of $d_{1,K}$ than adapted sites which at least once have hosted an lithium ion. Thus lithium ions can only visit those potassium sites with not too large values of $d_{1,K}$. (4) Lithium ions visiting a potassium site significantly attract the nearest oxygen. There is, however, only a partial adaption since the median of $d_{1,Li}$ is still 0.20 Å larger than the median for lithium sites. (5) In contrast, lithium sites only weakly adapt if entered by potassium ion. This is plausible from a chemical point of view because it is more difficult to compress the oxygen coordination shell rather than expanding it.

What can we learn from the properties of the mixed sites? A priori the mixed sites may have two different origins. First, they may reflect sites which during the first part of the 40ns were either lithium or potassium sites and in the second part changed their identity. This would give rise to a mixed average occupation. Second, they are never potassium or lithium sites but just have a structure which allows both ions to enter this site. Whereas the results in Fig. 5 do not allow us to distinguish between both scenarios the data in Fig. 6 clearly demonstrates that the second scenario is valid. If during some time interval the mixed sites would have acted as potassium sites the values of $d_{1,K}$ should be in the range of the values for potassium sites. Clearly, this is not the case. Thus a relevant number of site transitions from lithium to potassium type or vice versa cannot be seen.

The omitted corresponding plots for the second and third neighbors show gradually weaker displacements. The distance to the fourth oxygen neighbor, given in Fig. 7, finally does not show any effect of a change in the occupying species. The reaction of the network around a site to the nature of a visiting cation is thus very limited in range.

¿From these observations we would particularly like to stress that lithium and potassium sites only differ in the behavior of the first three oxygen atoms and that the properties of lithium sites do not change significantly, even if they are visited by potassium ions. This directly rationalizes the behavior, reported above, that the residence time of potassium in lithium sites is very short.

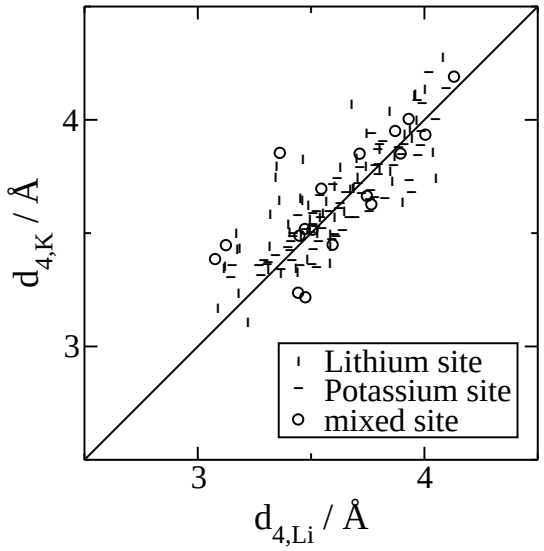


FIG. 7: Mean distances $d_{4,K}$ and $d_{4,Li}$ from mixed and adapted sites to the fourth oxygen neighbor.

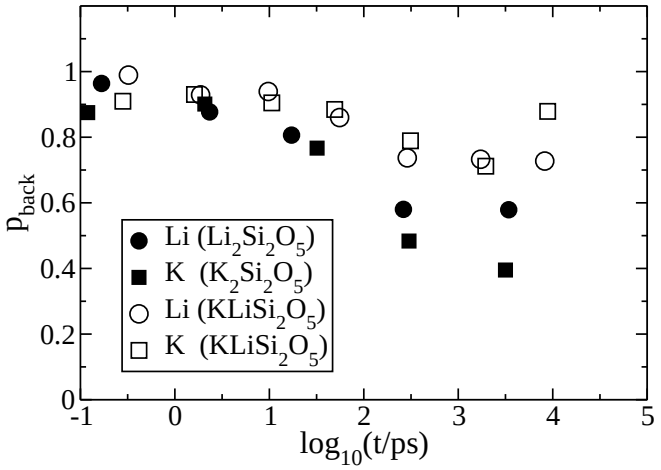


FIG. 8: Probability of direct backjumps A → B → C plotted against the average residence time for site B

.

D. Nearest-neighbor jumps

The local cation neighborhood of a cation determines, of course, the properties of nearest neighbor (nn) jumps. An important observable is the coordination number in the nearest neighbor (nn) shell, based on the partial pair correlation functions. Basically one counts the number of neighboring ions until the first minimum of the respective partial pair correlation functions. For Li-Li pairs we obtain 3.6 for K-K pairs 4.1 and for Li-K pairs 3.0. This clearly shows that, on the one hand, there is a slight tendency for clustering of like ions and, on the other hand, potassium ions have more neighbors than lithium ions. The latter point is a direct consequence of the fact that potassium has a larger ionic radius than lithium and thus

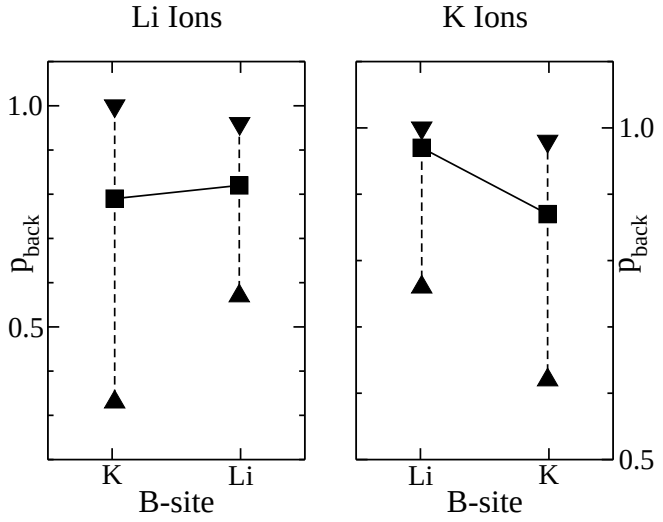


FIG. 9: Comparision of p_{back} out of matched and mismatched sites in the mixed–alkali system, for both lithium and potassium ions. The squares give the median of the distribution of one-site values, the triangles delimit the range including 34% of all sites both below and above the median.

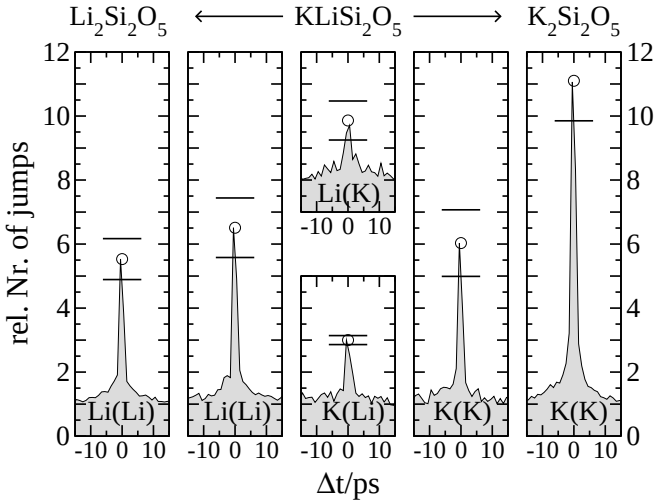


FIG. 10: Relative number of jumps from the neighboring sites a time Δt from a jump out of a given central site. In brackets the ion jumping at the center, in front the species jumping in response. The distribution is the average over those for any given central site.

has a larger nn sphere. It directly translates into the observation that also the number of nn sites is larger for potassium (8.1) than for lithium (7.1).

Of direct relevance for the dynamics are the number of nn sites which are accessible by a hopping process. It turns out that only ca. 60% and 40% of all nn sites were used as destinations for jumps by lithium and potassium ions, respectively. For the slowest sites, not all suitable neighbors may have been explored during the analyzed interval, especially in the case of potassium. But even considering this possibility, a significant fraction of nn sites must remain where the saddles are too large for a hop to occur. In the next step one may analyze the nature of those neighbors actually accessed during the simulation. It turns out that 70% of them are matching for the jumping ion. This value is significantly larger than the overall fraction of matching sites (ca. 47% for both species; see above). Matching sites are thus clearly favored as jump destinations.

Beyond the residence times the long-time dynamics is strongly influenced by the presence of correlated forward–backward jumps. To quantify this effect, we consider sequences of two jumps A $\rightarrow$ B $\rightarrow$ C performed by an ion. We define p_{back} as $p(C = A)$, the probability that an ion in a site B jumps back into the same site A from where it reached B. In Fig. 8, p_{back} is plotted against the average residence time of an ion in site B, $\tau_{res}(M_B)$.

In all systems, high probabilities are found for backjumps through sites B with short residence times, with values approaching 90%. p_{back} falls off for longer residences, down to 50% and 40% respectively for the lithium and potassium SA systems. These values are still high compared to the statistical probability of 15% corresponding to the average number of seven available neighbors in both cases. In the MA system, the curves level off to even higher values of p_{back} for long times, 65% and 70% for lithium and potassium. Generally, the probability of backjumps for any given residence time is higher than in the SA systems. The difference between the SA and the MA systems directly translates into the longer range of subdiffusive behavior (see above) and thus to a further decrease of the diffusion constant for the MA systems. This means that beyond the (minor) effect of longer waiting times it is to a large extent the increase of forward–backward correlations which gives rise to the slowdown in the MA system.

For a closer understanding of the backjump characteristics we have studied p_{back} for different sites. From Fig. 8 it is evident that short residence times are generally related to high backjump probabilities. This expectation is directly checked in Fig. 9. Therein the observed ranges for p_{back} out of lithium and potassium sites are opposed, for both species of ions. For potassium, the expected strong rise in p_{back} is found if B is a mismatched site. But the backjump probability of lithium ions is only slightly affected by the nature of the site B. This underlines our conclusions about the hopping properties of potassium ions. Whenever a potassium ion enters a mismatched site it can hardly enter because it is too difficult to create the necessary volume and immediately jumps back to the original site.

E. Dynamic correlation effects

So far we have analyzed the dynamic properties on a *single-particle* level. As discussed in the introduction an influence of *multi-particle* correlations is discussed in lit-

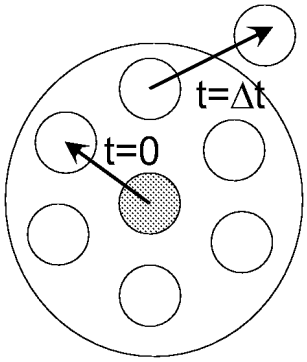


FIG. 11: Schematic of the type of correlated jump processes, considered in our analysis where four distinct sites as start and end points are required. The central site is shaded.

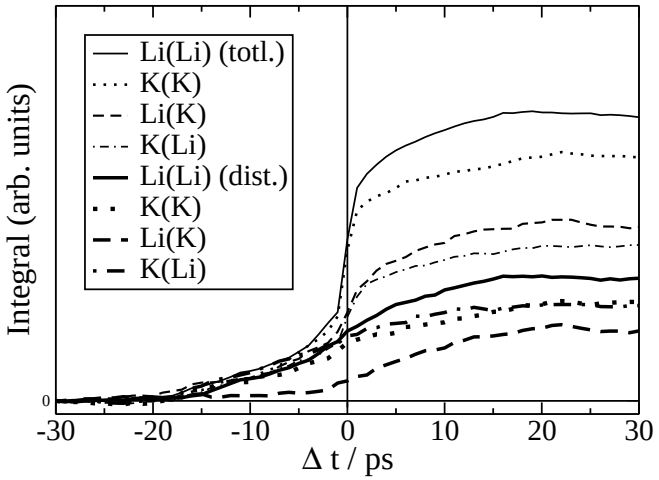


FIG. 12: Cumulative amount of additional jumps correlated with a jump at $t = 0$, for the mixed–alkali system. The importance of correlated jumps between four distinct sites is compared to the total extent of correlations including sequential movement as shown in Fig. 10.

erature as a possible mechanism to enable dynamic processes in MA systems. For example Habasaki demonstrated an additional slowdown of the lithium dynamics, if the potassium ions in a MA system were completely fixed[39]. The inferred correlations between jumps of different ions should be directly observable as an altered probability for a second jump shortly before or after one jump has happened. For each site, we have determined the number of jumps originating from one of its nn sites in dependence on the time difference Δt to a jump from the central site. Jumps by the same ion were ignored. The resulting distribution of jump probabilities was normalized and averaged over all sites. The value of one corresponds to the number of jumps from the neighbors happening without the influence of a jump from the central site, i.e. the behavior for long $|\Delta t|$. To gain an estimate of the scale of fluctuations in the results, this analysis was done separately for four subsequent pieces of the simulation of 10ns duration each. The distributions shown in Fig. 10 are the average over these four partial distributions. The error bars correspond to the standard deviation of the peak heights. The peaks show an increase in the number of nearby jumps by a factor of 5.5 and 11 for the lithium and potassium SA systems, respectively. For the correlations among like ions in the MA system, a factor of $6 - 6.5$ is found for both lithium and potassium. Correlations among jumps by unlike ions are weaker, but also present. The values are 3 for the lithium neighbors of a potassium ion, and also for potassium ions surrounding a lithium. In all cases, the maximum probability for correlated jumps is found at the time of the first jump, $\Delta t = 0$, and the peak is symmetrical. Careful inspection reveals that the peak consists of a narrow peak with half width close to 1 ps and a broad peak with with half width close to 5 ps. The latter peak will be discussed below.

The most simple scenario compatible with these findings is that a second ion jumps from a neighbor site into the site just vacated by the jump of the first ion. Indeed these correlations are reflected by the sharp peaks. But more complex correlations are also conceivable, which can generally be separated from the former kind by the additional condition that the two jumps use four distinct sites as start and end points; see Fig. 11 for a sketch.

The remaining correlations are responsible for the broad peaks in Fig. 10. For a quantitative analysis the maximum height is not suitable. Rather we show the integrals $\int_{-\infty}^{\Delta t} d\tau(peak(\tau) - 1)$ over the peaks; see Fig. 12. On the one hand, we integrate over the total peaks and, on the other hand, only over the remaining correlations if we use the additional four-site condition introduced above.

The total extent of four–site correlations given by the thicker lines is significant in all cases, amounting to ca. 50% of the total. To characterize the observed correlations, we determined the relative directions of the central jump and the correlated ones, given by the cosine of the enclosed angle. The directions of jumps using a common site are strongly correlated in all cases, as it is geometrically required. The jumps involved in four–site correlations are instead preferentially antiparallel in the SA systems. In the MA system, no correlation is discernible for the four–site correlations. Interestingly, the curve labelled Li(K), i.e. the probability of a lithium jump to follow a potassium jump, displays an asymmetry since it mainly increases for $\Delta t > 0$. Accordingly, the curve K(Li)shows the opposite asymmetry. Both observations imply that it is more likely that a jump of a potassium ion may trigger a jump of a lithium ion than vice versa. This observation is consistent our previous results that potassium sites are better suited for lithium ions than vice versa. A more detailed analysis, however, is necessary to further clarify the origin of this asymmetry.

In this analysis of correlations, all sites are taken into account with equal weight. When the sites are weighted according to the number of jumps taking place, the general effects remain, but their strength is greatly reduced.

One can thus conclude that dynamic correlation effects are particularly important in the vicinity of slow sites.

IV. DISCUSSION

The results favor an explanation of the mixed–alkali effect based on ionic sites that are specific for the different alkali species. The strongly bimodal distribution of occupation probabilities p_i^M shows that 90% of the ions reside in sites with a strong preference for one kind of ion. We have shown before that the location of the ionic sites is stable on the time scale of ionic transport[40]. It appears thus justified to treat the preference of a site for one species of ions as fixed over the course of the simulations. Possible effects of rare readaptions would still be incorporated via the treatment of "mixed" sites.

Trying to quantify the mixed–alkali effect in terms of properties of single sites or ions, the most direct contribution is observed in the distribution of residence times. The typical duration of residences in the predominant specific sites in the MA system is increased compared to the SA glasses. But this effect can account for only a small part of the observed mixed–alkali effect.

The increased probability for correlated forward–backward jumps will also add to the slowdown. As already in the SA systems the effect is strongest for sites with low residence times. Among them will be mismatching jump events, which generally have shorter τ_{res} than matching ones. But only for potassium ions this tendency translates into a further increase of p_{back}. The backjump probability of lithium is hardly affected by the adaption of the B site.

The maximum residence times and the oxygen coordination distances show that even strongly adapted sites can temporarily accommodate mismatching ions. Lithium again is favored, because it is apparently easier for the coordinating oxygens to approach than it is to recede from a site. But generally, both types of ions also visit mismatching sites, suggesting also some degree of interaction between the different species.

The data on two–ion correlations shows in fact that the dynamics of the different species in the mixed glass are not independent. The strongest correlations were observed for ions taking up sites just vacated by like ions, but foreign sites are also reached. Potassium ions will jump back with increased probability, but lithium ions are as likely to move on into a third place as from a matching site. For them, the correlations with the different ions should thus in fact facilitate transport.

As mentioned above the main difference between lithium and potassium is the ability of lithium to enter a potassium site without an immediate backjump, helped by the local oxygen environment. The reverse is strongly suppressed. This asymmetry is consistent with the larger mismatch evident in the residence times for potassium. For the present case of identical lithium and potassium concentration the transport is mainly via the matched sites for both species. In the limit where one species is very dilute the relevance of transport via mixed or mismatched sites may become important and may be relevant in particular for the smaller ion.

It may be interesting to compare the "first-principle" observations of this simulation work with the assumptions, used in the most recent version of the dynamic structure model[41,42] for the MA effect in solid glasses. Most ingredients like the presence of two different types of sites or the asymmetry between the smaller and the larger cation fully agree with our observations. There are, however, two aspects which are somewhat more speculative and where the present simulations yield new insight. Do sites change their character on time scales much shorter than the α relaxation time? Do so-called C$'$ sites exist? They are viewed as sites which after being vacated in the melt are somewhat smaller than the sites, actually visited by ions. From the simulations we have seen that on time scales up to the diffusive regime sites keep their identity so that the notion of a dynamic energy landscape is not supported by the simulation data. Furthermore there is no signature of possible C$'$ sites. They would be relevant if on the diffusion time scale transformations from C$'$ sites to regular sites and vice versa would occur. This would show up in a large number of sites, visited by the ions during the simulation run. Since the total number of sites, however, is just 8% larger than the number of ions there is basically no place for a large number of C$'$ sites being transformed to regular sites and vice versa.

In summary, a MA slowdown can be observed in the residence times as well as from increased likelihood of backjumps. Independent jump paths are favored. But the interception is not complete, as even mismatching sites are also accessible. Although actual cooperativity seems limited to the slowest ions, an enhancement of cation mobility is likely to follow. Together with the fast network dynamics in MA systems this rationalizes the enhanced dynamics in MA systems as compared to the predicted dynamics by assuming a dilution effect. Furthermore a significant asymmetry in the behavior of the smaller and the larger cation is observed. It will be interesting to see, whether an even closer analysis of the MA system, e.g. in terms of site and saddle energies, will be compatible with very recent explicit models of the dynamics in MA systems[43]. Furthermore a closer relation to ion-exchange experiments might be illuminating.

Acknowledgments

H. L. acknowledges funding by the german BMBF through the Fonds der Chemischen Industrie. This work was also supported by the DFG (SFB 458) . Furthermore we would like to thank A. Bunde, J. Horbach, M.D. Ingram, P. Maass, and H. Mehrer for stimulating discussions about this work.

* hlammert@uni-muenster.de
† andheuer@uni-muenster.de

[1] M. D. Ingram, Phys. Chem. Glasses **28**, 215 (1987).
[2] S. D. Baranowskii and H. Cordes, J. Chem. Phys. **111**, 7546 (1999).
[3] K. Funke, C. Cramer, and B. Roling, Glass Sci. Technol. **73**, 244 (2000).
[4] C. Cramer, S. Brunklaus, Y. Gao, and K. Funke, J. Phys.: Condensed Matter **15**, S2309 (2003).
[5] D. E. Day, J. Non-Cryst. Solids **21**, 343 (1976).
[6] G. Tomandl and H. A. Schaeffer, J. Non-Cryst. Solids **73**, 179 (1985).
[7] G. N. Greaves, S. J. Gurman, C. R. A. Catlow, A. V. Chadwick, S. Houde-Walter, C. Henderson, and B. Dobson, Philos. Mag. A **64**, 1059 (1991).
[8] J. Swenson, A. Matic, C. Karlsson, L. Borjesson, C. Meneghini, and W. S. Howells, Phys. Rev. B **63**, art. no. 132202 (2001).
[9] A. T. W. Yap, H. Förster, and S. R. Elliott, Phys. Rev. Lett. **75**, 3946 (1995).
[10] B. Gee and H. Eckert, J. Phys. Chem **100**, 3705 (1996).
[11] P. Jund, W. Kob, and R. Jullien, Philos. Mag. B **82**, 597 (2002).
[12] E. Sunyer, P. Jund, and R. Jullien, J. Phys.: Condens. Matter **15**, S1659 (2003).
[13] H. Lammert and A. Heuer, Phys. Rev. B **70**, 024204 (2004).
[14] A. Meyer, H. Schober, and D. B. Dingwell, Europhys. Lett. **59**, 708 (2002).
[15] A. Meyer, J. Horbach, W. Kob, F. Kargl, and H. Schober, Phys. Rev. Lett. **93**, 027801 (2004).
[16] S. Balasubramanian and K. J. Rao, J. Phys. Chem. **97**, 8835 (1993).
[17] J. Habasaki, I. Okada, and Y. Hiwatari, J. Non-Cryst. Solids **183**, 12 (1995).
[18] J. Habasaki, I. Okada, and Y. Hiwatari, J. Non-Cryst. Solids **208**, 181 (1996).
[19] B. Park and A. N. Cormack, J. Non-Cryst. Solids **255**, 112 (1999).
[20] P. Maass, A. Bunde, and M. D. Ingram, Phys. Rev. Lett. **68**, 3064 (1992).
[21] A. Bunde, M. D. Ingram, and P. Maass, J. Non-Cryst. Solids **172**, 1222 (1994).
[22] F. Berkemeier, S. Voss, A. W. Imre, and H. Mehrer, to be published (2004).
[23] M. D. Ingram, Glastech. Ber. Glass Sci. Technol. **67**, 151 (1994).
[24] P. W. S. K. Bandaranayake, C. T. Imrie, and M. D. Ingram, Phys. Chem. Chem. Phys. **4**, 3209 (2002).
[25] M. D. Ingram and B. Roling, J. Phys.: Condens. Matter **15**, S1595 (2003).
[26] R. Kirchheim, J. Non-Cryst. Solids **272**, 85 (2000).
[27] A. G. Hunt, J. Non-Cryst. Solids **255**, 47 (1999).
[28] H. Lammert, M. Kunow, and A. Heuer, Phys. Rev. Lett. **90**, 215901 (2003).
[29] J. Habasaki and Y. Hiwatari, Phys. Rev. B **69**, art. no. 144207 (2004).
[30] M. Vogel, Phys. Rev. B **70**, 094302 (2004).
[31] J. Dyre, J. Non-Cryst. Solids **324**, 192 (2003).
[32] K. Refson, Computer Physics Communications **126**, 310 (2000).
[33] J. Habasaki and I. Okada, Molec. Simul. **9**, 319 (1992).
[34] J. Habasaki and Y. Hiwatari, Phys. Rev. E **58**, 5111 (1998).
[35] R. D. Banhatti and A. Heuer, Phys. Chem. Chem. Phys. **3**, 5104 (2001).
[36] A. Heuer, M. Kunow, M. Vogel, and R. D. Banhatti, Phys. Chem. Chem. Phys. **4**, 3185 (2002).
[37] N. P. Bansal and R. H. Doremus, *Handbook of glass properties* (Academic Press, Orlando, 1986).
[38] M. Kunow and A. Heuer, cond-mat/0501589 (2005).
[39] J. Habasaki, K. L. Ngai, and Y. Hiwatari, J. Chem. Phys. **121**, 925 (2004).
[40] A. Heuer, H. Lammert, and M. Kunow, Z. Phys. Chem. **218**, 1429 (2004).
[41] A. Bunde, M. D. Ingram, and S. Russ, Phys. Chem. Chem. Phys. **6**, 3663 (2004).
[42] M. Ingram, R. Banhatti, and I. Konidakis, Z. Phys. Chem. **218**, 1401 (2004).
[43] R. Peibst, S. Schott, and P. Maass, arXiv:cond-mat/0503015 (2005).